Available online at www.sciencedirect.com
SCIENCE DIRECT®
C. R. Physique 6 (2005) 1129–1138
COMPTES RENDUS PHYSIQUE
http://france.elsevier.com/direct/COMREN/

MCAO for very large telescopes/OAMC pour les très grands télescopes

LINC-NIRVANA: MCAO toward Extremely Large Telescopes

W. Gaessler [a,*], C. Arcidiacono [b], S. Egner [a], T.M. Herbst [a], D. Andersen [a,e], H. Baumeister [a], P. Bizenberger [a], H. Boehnhardt [a,f], F. Briegel [a], M. Kuerster [a], W. Laun [a], L. Mohr [a], B. Grimm [a], H.-W. Rix [a], R.-R. Rohloff [a], R. Soci [a], C. Storz [a], W. Xu [a], R. Ragazzoni [a,b], P. Salinari [b], E. Diolaiti [b], J. Farinato [b], M. Carbillet [b], L. Schreiber [b], A. Eckart [c], T. Bertram [c], C. Straubmeier [c], Y. Wang [c], L. Zealouk [c], G. Weigelt [d], U. Beckmann [d], J. Behrend [d], T. Driebe [d], M. Heininger [d], K.-H. Hofmann [d], E. Nußbaum [d], D. Schertel [d], E. Masciadri [a]

[a] *Max-Planck Institut für Astronomie, Koenigstuhl 17, 69117 Heidelberg, Germany*
[b] *INAF Osservatorio Astrofisico di Arcetri, L.go E. Fermi, 5, 50125 Firenze, Italy*
[c] *1. Physikalisches Institut der Universität Köln, Zülpicher Straße 77, 50937 Köln, Germany*
[d] *Max-Planck-Institut für Radioastronomie, Auf dem Hügel 69, 53121 Bonn, Germany*
[e] *NRC Herzberg Institute of Astrophysics, 5071, West Saanich Road, Victoria V9E 2E7, British Columbia, Canada*
[f] *Max-Planck-Institut für Sonnensystemforschung, Max-Planck-Straße 2, 37191 Katlenburg-Lindau, Germany*

Available online 10 January 2006

Abstract

LINC-NIRVANA is a Fizeau (imaging) interferometer exploiting the full spatial resolution of a 23 m class telescope in the combined beam of the Large Binocular Telescope supported through Multi-Conjugated Adaptive Optics (MCAO). By means of science cases, we show how LINC-NIRVANA takes advantage of the MCAO, increasing the sky coverage of the instrument and the field of view for the Fringe and Flexure tracker. We introduce the MCAO system of LINC-NIRVANA in detail, which in a first step will be installed with two deformable mirrors per arm and has the provision to be upgraded with a third mirror. The MCAO system implements several novel concepts proposed for extremely large telescopes, such as layer oriented MCAO, optical co-adding of guide stars, or Multiple Field of View sensing. LINC-NIRVANA will demonstrate some of the concepts for the first time on sky. ***To cite this article: W. Gaessler et. al., C. R. Physique 6 (2005).***

Résumé

LINC-NIRVANA : MCAO vers les télescopes extrêmement grands. LINC-NIRVANA est un interféromètre de Fizeau (formation image) explorant la pleine résolution spatiale d'un télescope de classe de 23 m dans le faisceau combiné du LBT soutenu par le systeme optique adaptatif Multi-Conjugué (MCAO). Au moyen de cas de science, nous montrerons comment LINC-NIRVANA tire profit du MCAO, qui augmente la couverture de ciel de l'instrument et le champ visuel du traqueur de frange et de flexure. Nous présenterons le système de MCAO de LINC-NIRVANA en détail, qui dans une première étape sera installé avec deux miroirs deformable par bras et a la disposition dêtre prolongé avec un troisiéme miroir plus tard. Le système de MCAO met en application plusieurs concepts nouveau proposés pour les télescopes extrêmement grands, comme MCAO

* Corresponding author.
E-mail address: gaessler@mpia.de (W. Gaessler).

1631-0705/$ – see front matter
doi:10.1016/j.crhy.2005.11.005

orienté par couche, Co-s'ajouter optique du guide tient le premier rôle ou champ visuel multiple senseur. LINC-NIRVANA les démontrera pour la premiére fois sur le ciel. ***Pour citer cet article : W. Gaessler et. al., C. R. Physique 6 (2005).***

Keywords: AO; MCAO; Interferometry; Fizeau; LBT

Mots-clés : AO ; MCAO ; Interférométrie ; Fizeau ; LBT

1. Introduction

The Large Binocular Telescope (LBT) [1] is being built on Mt. Graham in Arizona, USA. It has two 8.4 m lightweight honeycomb mirrors, which will be combined into one focus after the full deployment of the telescope in late 2007. The telescope uses Adaptive Secondary Mirrors (ASM) to correct for atmospheric turbulence. The telescope optics are Gregorian style, providing a prime focus below the secondary, where one can place retro-reflectors or a calibration source to support ASM calibration.

LINC-NIRVANA (LN) will be one of two instruments taking advantage of the combined beam at LBT. LN will have a resolution of a 23 m telescope in one direction and that of a 8.4 m telescope in the other (see Fig. 1). Observations of the same target at different parallactic angles can be used to reconstruct an image with the full resolution of a 23 m telescope in all directions [2].

2. Science with LN

The gain for an instrument in the combined beam of the LBT is the increase in sensitivity, due to the collection area of two 8.4 m mirrors, and the spatial resolution of a 23 m telescope. An overview of some science cases and their requirements is given in Table 1.

LN goals are not only on higher spatial resolution and sensitivity but also on a larger field of view and larger sky coverage compared to other interferometric instruments. These features are especially important for extra galactic science and astrometry. Due to the ratio between single dish diameter and baseline at LBT, observers can fully sample the uv plane with LN in a small number of exposures. This allows true imaging of extended and complex galactic or extra galactic sources, such as star forming regions, disks, jets or galaxy morphology. LN will not provide the same contrast as an extreme AO system aboard a 10 m class telescope, but compensates this partially through higher spatial resolution. The advantage will vary from target to target and the class of objects for which LN can gain is given here only as a general guideline.

One of the major science cases is the study of extragalactic populations out to 20 Mpc. Fig. 2 shows a simulation of the nearby galaxy NGC 4535 in the K band artificially red shifted to $z = 1$. LN still resolves star clusters at $z = 1$, while neither HST nor a diffraction-limited 8 m telescope can do this. MCAO will give only partial correction. An instrument at a 8 m class

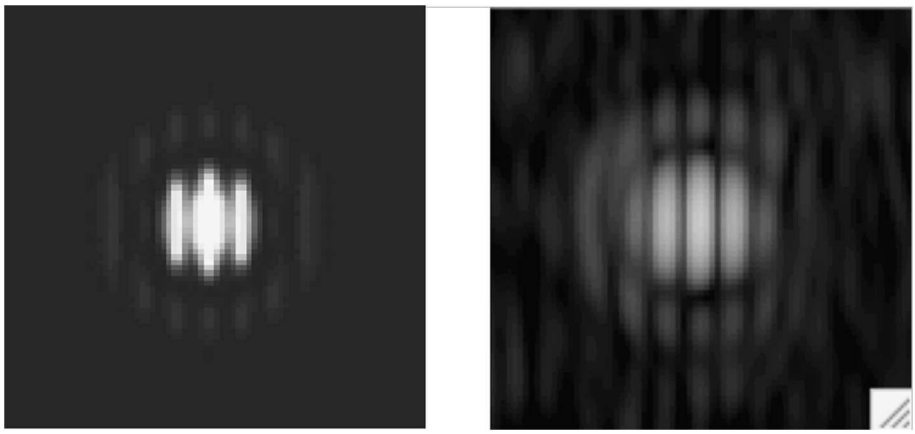

Fig. 1. Simulation of an instantaneous point spread function of a point source for LINC-NIRVANA in K-band. The resolution of a 23 m telescope is obtained in the horizontal direction and that of an 8.4 m telescope in the vertical direction. At the left is shown an ideal PSF with no aberrations. On the right is a PSF with 350 nm residual wavefront error and a strehl ratio of 0.28, a typical value we expect to achieve with LN.

Table 1
Extra galactic and galactic science cases and their requirements

Science cases (extra galactic)	F	R	S
Cosmological Parameters (SN Ia)	X		X
Galaxy Formation/Morphology	X	X	X
Extra Galactic Stellar Populations	X	X	X
Dark Matter (Tidal streams, ...)	X		
Astrometry (Black Hole masses, ...)	X	X	
Science cases (galactic)			
Star formation	X	X	
Circumstellar disks	(X)	X	
Exo-planets with astrometry	X	X	
Exo-planets with direct imaging		X	

Three requirements are distinguished: field of view (F), spatial resolution (R) and sensitivity (S).

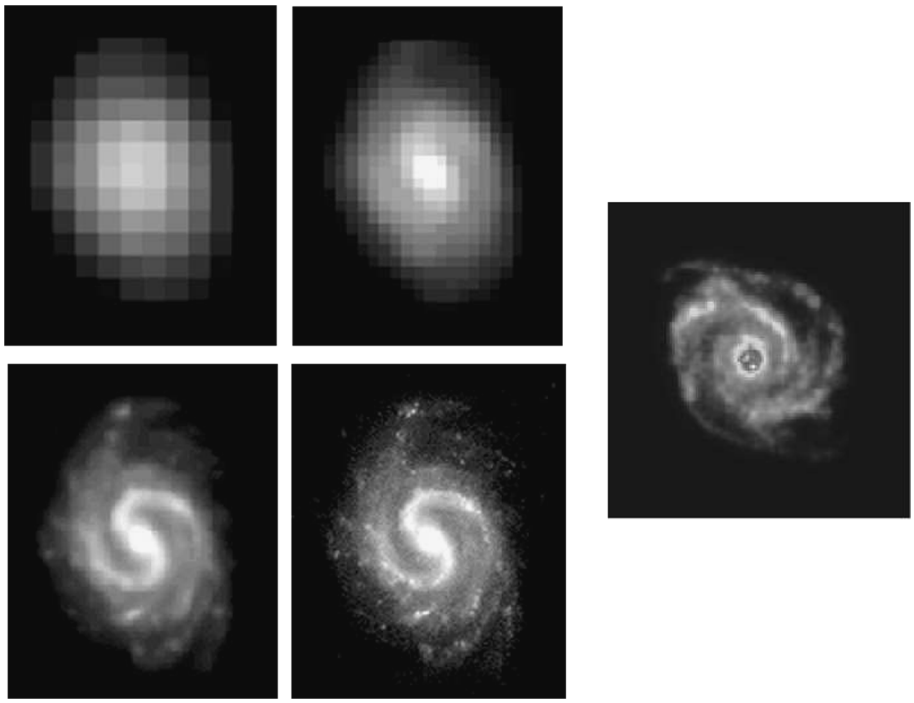

Fig. 2. NGC 4535 at K artificially red shifted to $z = 1$ with seeing-limited resolution of $0.4''$ in the upper left, HST resolution of $0.2''$ in the upper right, diffraction-limited resolution of a 8.4 m telescope at about $0.06''$ in the lower left and the diffraction limited fully reconstructed resolution with LN of $0.02''$ in the lower right. The picture on the right side shows a simulation for LN of a different galaxy using only partial MCAO correction.

telescope faces the same problem, but due to the better resolution, LN reveals the structure of the galaxy, even with partial MCAO correction, as shown in the simulation on the right of Fig. 2.

For galactic astronomy, the search for planets is very popular. With the resolution of LN the search for Jupiter-like planets through astrometric wobble out to 100 pc can be done. The field of view increases the likelihood of reference stars for such astrometric measurements and the higher resolution gives a better precision, increasing the distance to which targets can be probed.

3. The instrument

LN is a Fizeau (imaging) interferometer placed in the rear bent combined focus of the LBT. It occupies a space 5.5 m wide, 4.9 m deep and 4.4 m high. Fig. 3 is a computerized rendering of LN and its components.

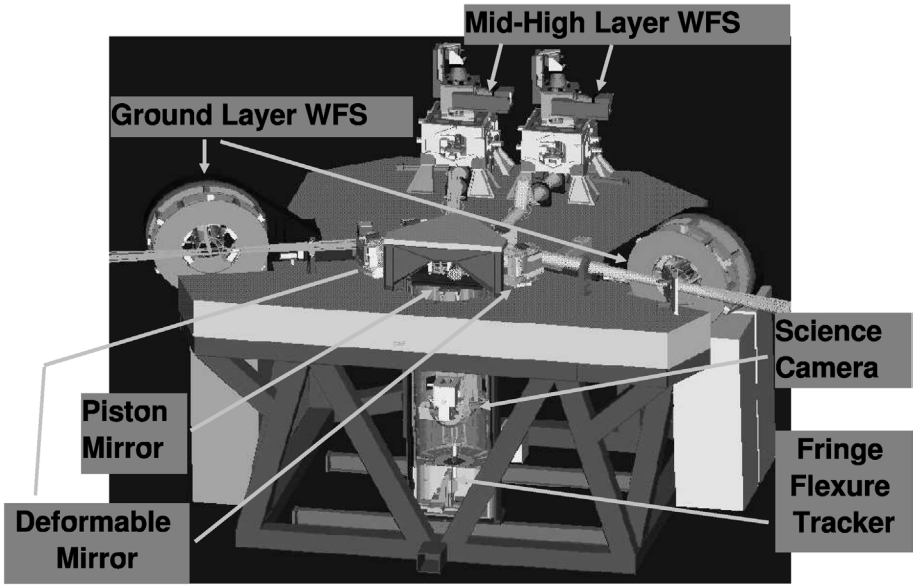

Fig. 3. Overview of LINC-NIRVANA seen from the front. All the major components are named. The dimensions of the instrument are 5.5 m × 4.9 m × 4.4 m ($W \times D \times H$).

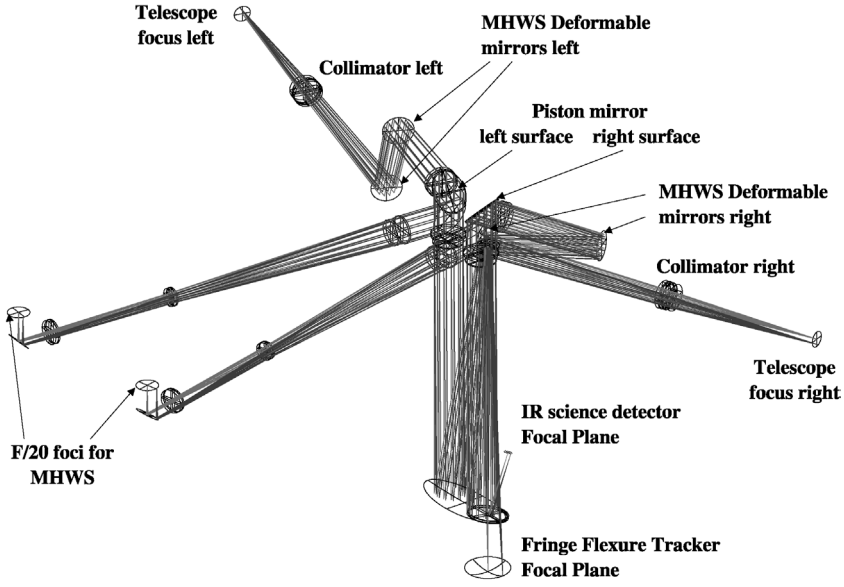

Fig. 4. Optical layout of LINC-NIRVANA seen from the right back side.

The heart of the instrument is a cryostat comprising an infrared science camera and a fringe and flexure tracker system (FFTS). The science camera will have a FoV of $10'' \times 10''$ and is sensitive in the J, H and K photometric bands. The pixel scale is 5 mas/pixel to have Nyquist sampling over all wavelength range. The spatial resolution, as given by λ/D of a 23 m diameter telescope, is 11 mas in J-band and 20 mas in K-band. The FFTS operates at the same wavelengths. It measures the optical path difference between the right and the left telescope arm and corrects the difference by moving the piston mirror, a device existing of two folding mirrors mounted on one mechanical unit to direct the left and right beam into the cryostat (see Fig. 4). The differential piston is calculated through a PSF fitting algorithm using non-linear least square optimization [3]. The FFTS guide star is selected within a field of $1.5' \times 1'$. To allow such a wide field for fringe tracking, a Multi-Conjugated Adaptive Optic (MCAO) system is implemented. The deformable mirrors used are not constrained at the edges, and real piston neutral

modes can be applied. The non linearity of piezo actuators will be corrected with a lookup table. Hence, the remaining piston, introduced by the Adaptive Optics, is reduced to the actuator hysteresis, which is less than $\lambda/25$ and therefore negligible [4].

4. The MCAO system

LN has separate but identical MCAO systems for the left and right 8.4 m mirror of the LBT. The scheme of the MCAO for one of the 8.4 m mirrors is shown in Fig. 5. The outer annulus from $1'$ to $3'$ radius is used by the Ground Layer Wavefront Sensor

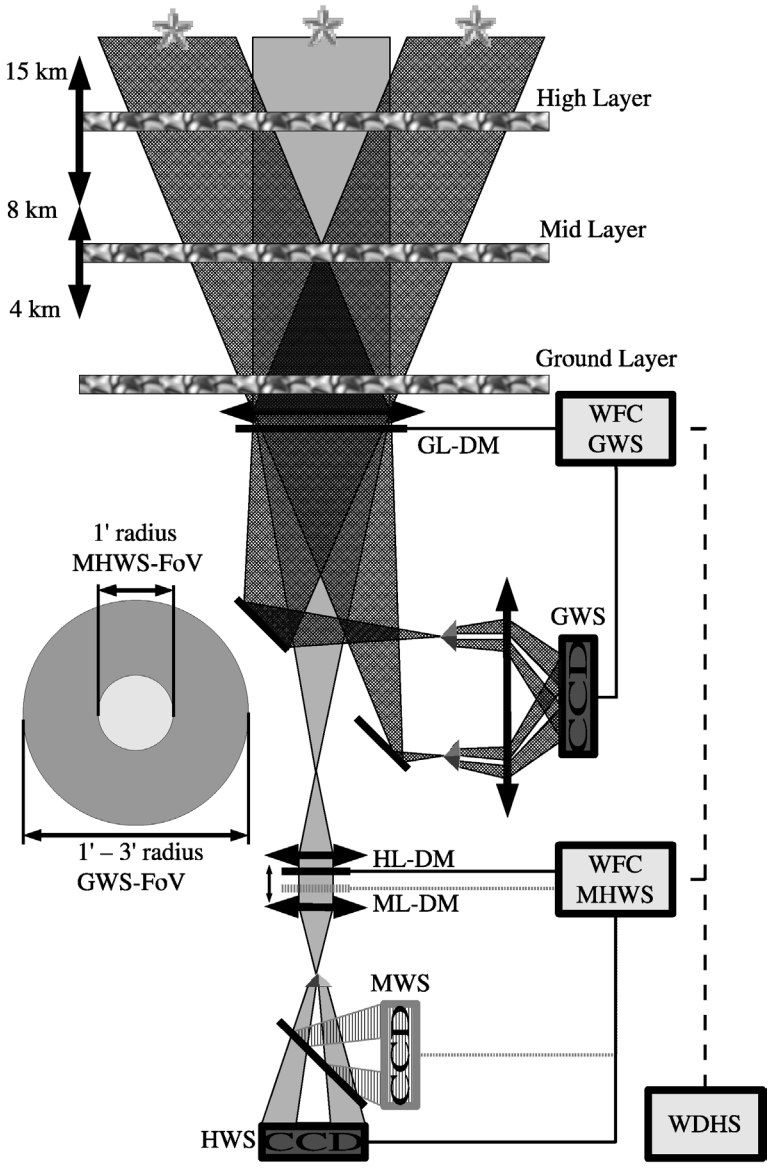

Fig. 5. Sketch of the LN MCAO for single 8.4 m dish. The outer annulus from $1'$ to $3'$ radius is used by the Ground Layer Wavefront Sensor (GWS). Up to 12 Natural Guide Stars (NGS) can be optical co-added. The central Field of $1'$ radius is used with up to 8 NGS by the Mid-High Layer Wavefront Sensor (MHWS), which splits the light to the Mid Wavefront Sensor (MWS) CCD and the High Wavefront Sensor CCD (HWS). Both Sensors have their own Wavefront Computer (WFC) running the control loop independently. A Wavefront Data Handling System (WDHS) optimizes the control loops and off-loads modes from one to the other to avoid saturation. The High Layer and Mid Layer Deformable Mirrors (HL-DM,ML-DM) can be adjusted together to their conjugated altitude, HL-DM between 8 and 15 km, ML-DM between 4 and 8 km, respectively. In the first step only HWS and GWS are implemented. Therefore the MWS and its DM are only shaded in this picture.

(GWS). Up to 12 Natural Guide Stars (NGS) can be optically co-added. The central Field of $1'$ radius is sampled with up to 8 NGS by the Mid-High Layer Wavefront Sensor (MHWS), which splits the light to the Mid Wavefront Sensor (MWS) CCD and the High Wavefront Sensor CCD (HWS). The number of guide stars is constrained by mechanics, and by the number of stars to be found over a suitable magnitude range in the FoV of each sensor, without losing too much sky coverage [12]. Each wavefront sensor has a corresponding deformable mirror. The GWS runs the facility ASM with its 672 actuators, a device designed to deliver strehl of better than 0.5 in the R-band at $0.7''$ seeing [5]. The MHWS uses 349 actuator piezostack deformable mirrors placed on the instrument bench, which are oversampling the needs for J, H, K-band observations by far, but keep the provision to extend the instrument to visible wavelengths without changing the AO system. The Mid Layer Wavefront Sensor can be conjugated to any altitude between 4 and 8 km, while the High Layer Wavefront Sensor can be focused in the range of 8 to 15 km. For technical simplification, the mid and high layer DM can only be moved together. How this is accomplished is described in more detail in Section 5. The GWS samples the diameter of the pupil with 48 pixels, chosen to match the Fried parameter of 0.2 m for a seeing of $0.7''$ in the visible. The MHWS samples a single star pupil with 18 pixels at 0 km altitude, increasing to 38 pixels at 15 km. Each pixel corresponds to one sub-aperture.

In the first implementation, only the ASM and one DM for the high altitude will be installed per arm. The third DM is planned for a later upgrade or a single telescope three deformable mirror MCAO demonstration. Also, the third sensor camera will be implemented later. Hence, in the first step the MHWS with one DM is just a simple high layer wavefront sensor.

The MCAO system implements and tests for the first time several novel features, which are also proposed for AO on Extremely Large Telescopes:

- Pyramid Wavefront Sensing [6];
- Optical Co-adding of Guide Stars [8];
- Layer Oriented Multi-Conjugated Adaptive Optics [8];
- Multiple Field of View Wavefront Sensing [7].

The Pyramid Sensor (PS) has advantages in operational aspects as well as in performance, for example the size of the sub-apertures can be tuned to the actual atmospheric conditions just by re-binning the CCD. The sensitivity of the PS increases in the diffraction-limited regime for the sensing wavelength, and the PS is also less noisy in correcting low order modes than a Shack–Hartmann Sensor [15].

Since the PS is a pupil wavefront sensor, the light of several guide stars can be co-added optically, so that the magnitude of each single guide star can be fainter. The guide stars should be selected within the same magnitude range. If one star is brighter than all the others, it will dominate the wavefront measurement [12].

In combination with PS and optical co-adding, the layer-oriented MCAO approach is a choice to simplify the control architecture, especially if it is done in cascade, as in LN with the GWS and MHWS. The layer-oriented MCAO approach has, in general, less computational demands than star-oriented MCAO, and therefore eases the need of calculation power.

The final concept included in the MCAO is the Multiple Field of View Sensing. The GWS use a different and larger field than the MHWS. With increasing field, the number of possible guide stars gets larger, which results in greater sky coverage.

LN uses the MCAO system mainly to increase the sky-coverage and the field of view of the FFTS. The possibility to use the full AO corrected $2'$ for the science camera is not implemented, because the size of the cryostat would increase and the cost for the number of detectors needed to cover such an area, keeping the sampling for the full resolution, is still too high.

5. Altitude conjugation

MCAO provides optimal correction with conjugation of the DM to the effective altitude of the turbulence. This is true for both the layer oriented and star oriented approaches. Any mis-placement in altitude of the DM, and in the layer oriented case, also of the sensors, smoothes out the spatial frequencies of the higher orders as shown by [13] or [14]. We are conducting SCIDAR measurements at Mt. Graham to understand the behavior of the turbulence layers at the site. Preliminary results are shown in Fig. 6. The optimal conjugated altitude of turbulence for two mirrors was calculated, following the method described by Tokovinin et al. [13], optimizing for the maximum isoplanatic patch. The turbulence for the first mirror was permanently just above the ground, while within the night the altitude for a second mirror was on average at 14.8 km but varying over a range of 7 to 22 km. An optimization for the maximum isoplanatic patch leads to higher altitudes as one for the maximum average strehl in the science field. The average isoplanatic patch with a fixed DM at a fixed altitude of 14.8 km would be $8.5''$ in V-band, $25.8''$ in J-band and $50.9''$ in K-band, respectively, for these measurements. Moving the DM to the optimized altitude increases the isoplanatic patch to $12.9''$ in V-band, $38.7''$ in J-band and $76.3''$ in K-band. In addition to the atmospheric changes of the layer heights, one has to consider, that observing at lower elevation, the distance to the turbulence layer increases. Therefore, to adjust the distance to the layers and reduce the degradation of the isoplanatic patch, the DM are placed on translation stages.

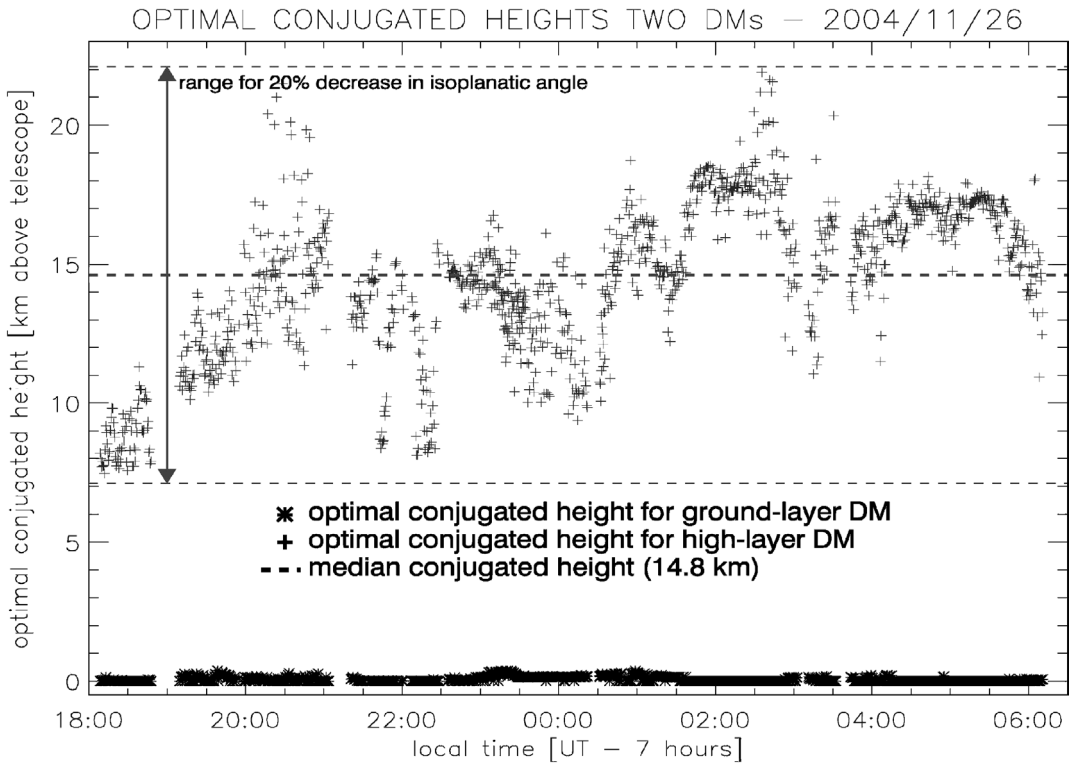

Fig. 6. The change in optimal conjugated heights of the turbulence for two deformable mirrors. The turbulence of the first mirror is permanently fixed just above the ground, while the optimal conjugated height of turbulence for the second mirror varied over a range of 15 km within one night.

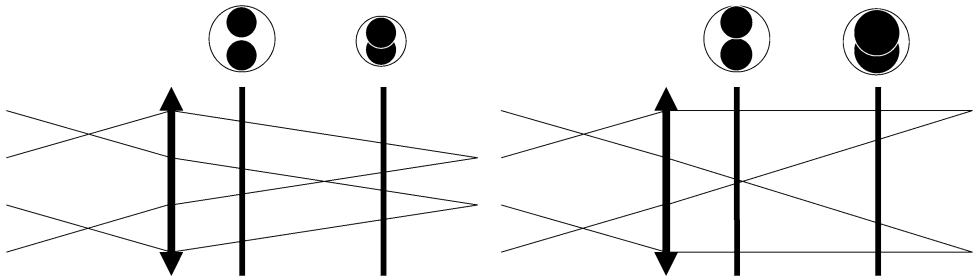

Fig. 7. Left: Sketch of a conventional collimator; right: sketch of a constant envelope collimator.

This introduces some technical complications, since the DM are normally placed within a collimated beam which changes its outer envelope over the collimator length. Such conventional DM are shown in Fig. 7, left picture. The meta-pupil of a conventional collimator changes size, while the pupil of each guide star keeps its size. Moving a DM in such a collimator would lead to a loss in correction elements, since the size of the DM will not change. Therefore, we use a constant envelope collimator as shown in Fig. 7, right picture, which keeps the meta-pupil constant but changes the size of the guide star pupil.

6. Sky coverage

Exhaustive simulations [9,10] on the overall sky coverage for LN were performed to verify the expected improvement. The input parameters for the simulation were taken from [11]. A seven layer atmosphere as measured at Paranal (North Chile) is assumed. The average seeing is set to $0.43''$ in the K-band, which is equivalent to $0.7''$ in the R-band. The sampling time ranges from 2 to 40 msec, depending on the overall co-added guide star brightness. Only the guide stars related to the fields of each

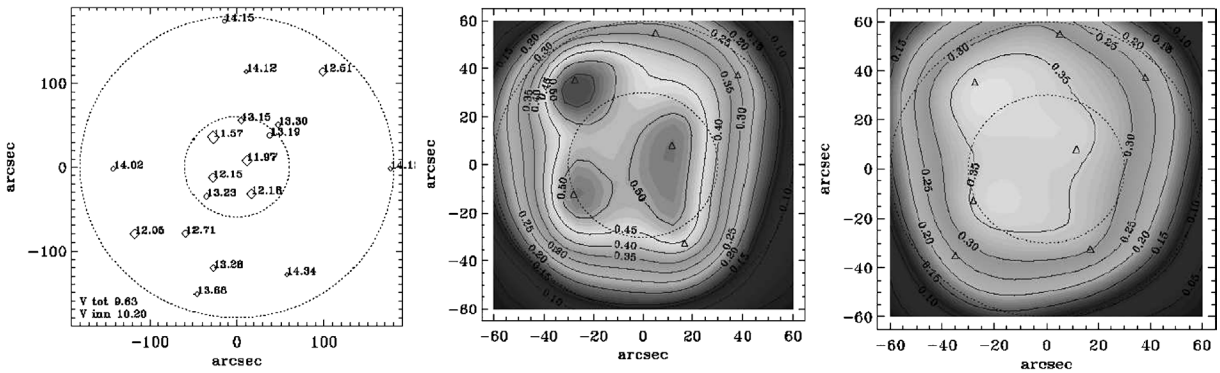

Fig. 8. Strehl evaluation for the bright guide star case (from [10]). Left: catalog map of the guide stars. The selected guide stars are marked with a diamond and their magnitude in R-band is given. The inner circle is the FoV of the MHWS and the outer circle the FoV of the GWS. Middle: Strehl map for the single telescope MCAO system using the MHWS and GWS. The contour lines and different grey scales define the Strehl ratio, the triangles mark the guide stars and the dotted rings the FoV of the MHWS and GWS, respectively. Right: same kind of Strehl map as in the middle, but for the combined interferometric beam.

Table 2
Summary of the sky coverage simulation for the 3 different fields at each place of test

Case	NGP	SGP	Galactic center
On axis	48.00%	25.00%	99.00%
$1'$ FoV	38.00%	17.00%	97.00%
$2'$ FoV	25.00%	13.00%	99.00%

A field was considered as covered if its average strehl ratio exceeded 10%.

sensor are co-added. The exposure time for each image is 1 second. The sensing wavelength is 0.75 μm while the science wavelength is chosen as 2.2 μm. Selected examples with bright and faint guide stars for the single arm and the interferometric configuration are studied. The result for the case of bright guide stars appear in Fig. 8. The guide stars are randomly distributed over the field. Such cases can be found at Galactic Latitude up to 20 degrees. The relevant simulation of the interferometric beam shows a quite homogeneous strehl of 0.35 in average over the central $2'$ which is used by the FFTS and science camera.

The sky coverage estimate was made using the USNO-B catalog by sampling a 1×1 degree field at the Galactic Center, the North Galactic Pole (NGP) and the South Galactic Pole (SGP)with a grid of 32×32 points separated by $101''$ from each other. A Strehl map was calculated for each point of the grid. The distance between the guide stars was not closer than $20''$ for the MHWS and $30''$ for the GWS, caused by the fact that the pyramids and their holders have finite dimension. The maximum difference in luminosity was 3 magnitudes as recommended in [12]. The Strehl maps were evaluated for three different science field sizes: a few arcseconds on-axis, $1'$ FoV and $2'$ FoV. Only maps which show more than 10% average Strehl ratio in the corresponding field size were counted in the sky coverage calculation. The magnitude of the co-added guide stars was 14, while stars down to 19th magnitude in visible could be chosen. The result is summarized in Table 2. Full sky coverage can be obtained at the Galactic Center, while it is in the worst case 25% at the NGP and 13% at the SGP, considerably more than the 5% value typical for single star AO.

Fig. 9 shows the distribution of the average strehl over a $2'$ FoV at the South Galactic Pole (SGP), the North Galactic Pole (NGP) and the Galactic Center (GC). The sky coverage is still about 5% at the NGP and SGP for a Strehl of 0.2 and there is nearly full sky coverage at the GC for a Strehl up to 0.3. The low Strehl does not affect the fringe pattern, which depends on the coherence length, but the fringe contrast. The speckle noise of the residual wavefront error will decrease the signal to noise ratio for the fringe tracking. The algorithm is tested to be robust against such noise [16].

7. Conclusion

LN will exploit the interferometric capabilities of the LBT over a FoV of $10'' \times 10''$ in true imaging mode. It is currently the only instrument planned for an interferometer providing such FoV. The advantages of LN are higher sensitivity and higher spatial resolution over a larger FoV. To achieve this goal LN will use several novel techniques of AO, such as pyramid wavefront sensors, optical co-adding, layer oriented MCAO and Multiple FoV sensing, which are also proposed for ELT. The MCAO can

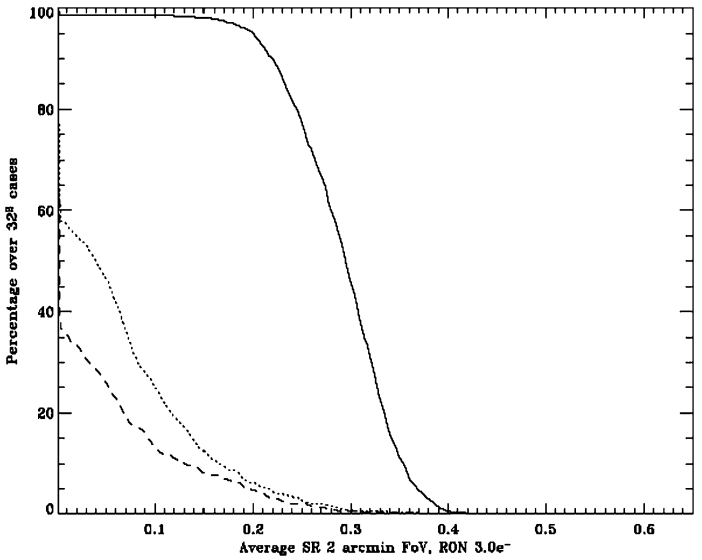

Fig. 9. Distribution of the average Strehl ratio over a 2 arcmin FoV at the SGP (dashed line), NGP (dotted line) and the Galactic Center (solid line) (from [10]).

be adjusted to the optimal heights of turbulence to increase the isoplanatic patch. The system increases the sky coverage as shown by extensive simulations. The full MCAO system and its constraints are relaxed by having separate sensors for each eye and using them independently and in cascade for the ground and high layers. Even if one of the sensors fails, the system will continue with reduced performance. Nevertheless, LN will be a complex, difficult to operate instrument. Some techniques, such as Multiple FoV sensing or the FFTS algorithm, will be implemented for the first time. Such a risk is mitigated by the optomechanical design, which is modular and kept open to a step-by-step implementation and future extensions. A carbon fiber bench is chosen to keep the intrinsic stiffness of the instrument high and flexure effects low. Damping of vibrations from the telescope will be done through the structure and material selection of the bench, and even the provision of an active damping system is kept open. Currently, vibration measurements are conducted at the telescope to understand better the reality LN will have to fight with. The implementation of the instrument will be in several steps, starting from interferometry with a single star AO, than testing single eye GLAO and then MCAO, and finally using the interferometry with MCAO. After proving the concepts and getting LN into a smooth operational state, upgrades to more deformable mirrors, a larger science field or integral field spectroscopy will be considered. LN makes use of the LBT as a (masked) 23 m class telescope. Hence, the instrument faces problems similar to those confronting instruments for the next generation of Extremely Large Telescopes. In many ways, LN is a testbed for such instruments.

Acknowledgements

LINC-NIRVANA is funded through the Wolfgang Paul Prize of the Alexander von Humboldt Foundation, the Max-Planck Society, BMBF Verbundforschung, INAF and the University of Köln. A prototype of the Multiple FoV sensor is funded through the FP6 JRA1 of OPTICON.

References

[1] J. Hill, P. Salinari, The Large Binocular Telescope Project, in: Proceedings of the SPIE Conference, vol. 5489, 2004, pp. 603–614.
[2] M. Carbillet, S. Correia, P. Boccacci, M. Bertero, Restoration of interferometric images. II. The case-study of the Large Binocular Telescope, A&A 387 (2002) 744–757.
[3] T. Bertram, C. Straubmeier, D.R. Andersen, C. Arcidiacono, U. Beckmann, A. Eckart, T.M. Herbst, The LINC-NIRVANA fringe- and flexure-tracker: PSF- and atmospherical differential piston simulations and determination algorithm, in: Proceedings of the SPIE Conference, vol. 5491, 2004, p. 167.
[4] S.E. Egner, W. Gaessler, T.M. Herbst, R. Ragazzoni, D.R. Andersen, H. Baumeister, P. Bizenberger, H. Boehnhardt, S. Ligori, H.-W. Rix, R. Soci, R.-R. Rohloff, R. Weiss, W. Xu, C. Arcidiacono, J. Farinato, E. Diolaiti, P. Salinari, E. Vernet-Viard, A. Eckart, T. Bertram, C. Straubmeier, LINC-NIRVANA: the single arm MCAO experiment, in: Proceedings of the SPIE Conference, vol. 5490, 2004, p. 175.

[5] M. Carbillet, S. Esposito, A. Riccard, Numerical simulations studies for the first-light adaptive optics system of LBT, in: Proceedings of the SPIE Conference, vol. 5490, 2004, p. 153.
[6] R. Ragazzoni, Pupil plane wavefront sensing with an oscillating prism, J. Mod. Opt. 43 (1996) 289.
[7] R. Ragazzoni, E. Diolaiti, J. Farinato, E. Fedrigo, E. Marchetti, M. Tordi, D. Kirkman, Multiple field of view layer-oriented adaptive optics. Nearly whole sky coverage on 8 m class telescopes and beyond, A&A 396 (2002) 731–744.
[8] R. Ragazzoni, Adaptive optics for giant telescopes: NGS vs. LGS, in: ESO Conference and Workshop Proceedings, vol. 57, 1999, p. 175.
[9] C. Arcidiacono, E. Diolaiti, R. Ragazzoni, A. Baruffolo, A. Brindisi, J. Farinato, E. Vernet, Sky coverage and SR uniformity in Layer-Oriented MCAO, in: Proceedings of the SPIE Conference, vol. 5189, 2003, pp. 169–180.
[10] C. Arcidiacono, Multi-conjugated adaptive optics for large telescopes, PhD Thesis, University Florence, 2005, submitted for publication.
[11] M. Le Louarn, N. Hubin, M. Sarazin, A. Tokovinin, New challenges for adaptive optics: extremely large telescopes, Mon. Not. R. Astron. Soc. 317 (2000) 535–544.
[12] E. Marchetti, R. Ragazzoni, E. Diolaiti, Which range of magnitude for Layer Oriented MCAO?, in: Proceedings of the SPIE Conference, vol. 4839, 2002, pp. 566–577.
[13] A. Tokovinin, M. Le Louarn, M. Sarazin, Isoplanatism in a multiconjugate adaptive optics system, JOSA A17 (10) (2000) 1819.
[14] E. Diolaiti, R. Ragazzoni, M. Tordi, Closed loop performance of a layer-oriented multi-conjugated adaptive optics system, A&A 372 (2001) 710–718.
[15] C. Vérinaud, On the nature of the measurements provided by a pyramid wave-front sensor, Optical Commun. 233 (1–3) (2004) 27–38.
[16] T. Bertram, LINC-NIRVANA FDR Chapter 5.1 FFTS simulations, http://www.mpia.de/LINC/index.html, 2005.